Specific Local Cardiovascular Changes of N^{ε}-(Carboxymethyl)lysine, Vascular Endothelial Growth Factor, and Smad2 in the Developing Embryos Coincide With Maternal Diabetes–Induced Congenital Heart Defects

Pauline A.M. Roest,[1] Daniël G.M. Molin,[2] Casper G. Schalkwijk,[3] Liesbeth van Iperen,[1] Parri Wentzel,[4] Ulf J. Eriksson,[4] and Adriana C. Gittenberger-de Groot[1]

OBJECTIVE—Embryos exposed to a diabetic environment in utero have an increased risk to develop congenital heart malformations. The mechanism behind the teratogenicity of diabetes still remains enigmatic. Detrimental effects of glycation products in diabetic patients have been well documented. We therefore studied a possible link between glycation products and the development of congenital cardiovascular malformations. Furthermore, we investigated other possible mechanisms involved in this pathogenesis: alterations in the levels of vascular endothelial growth factor (VEGF) or phosphorylated Smad2 (the latter can be induced by both glycation products and VEGF).

RESEARCH DESIGN AND METHODS—We examined the temporal spatial patterning of the glycation products N^{ε}(carboxymethyl)lysine (CML) and methylglyoxal (MG) adducts, VEGF expression, and phosphorylated Smad2 during cardiovascular development in embryos from normal and diabetic rats.

RESULTS—Maternal diabetes increased the CML accumulation in the areas susceptible to diabetes-induced congenital heart disease, including the outflow tract of the heart and the aortic arch. No MG adducts could be detected, suggesting that CML is more likely to be indicative for increased oxidative stress than for glycation. An increase of CML in the outflow tract of the heart was accompanied by an increase in phosphorylated Smad2, unrelated to VEGF. VEGF showed a time-specific decrease in the outflow tract of embryos from diabetic dams.

CONCLUSIONS—From our results, we can conclude that maternal diabetes results in transient and localized alterations in CML, VEGF expression, and Smad2 phosphorylation overlapping with those regions of the developing heart that are most sensitive to diabetes-induced congenital heart disease. ***Diabetes*** **58: 1222–1228, 2009**

From the [1]Department of Anatomy and Embryology, Leiden University Medical Centre, Leiden, the Netherlands; the [2]Department of Vascular Physiology, Cardiovascular Research Institute Maastricht, Maastricht University, Maastricht, the Netherlands; the [3]Department of Internal Medicine, Maastricht University, Maastricht, the Netherlands; and the [4]Department of Medical Cell Biology, Uppsala University Biomedical Centre, Uppsala, Sweden.

Corresponding author: Adriana C. Gittenberger-de Groot, acgitten@lumc.nl.

Received 23 July 2007 and accepted 26 January 2009.

Published ahead of print at http://diabetes.diabetesjournals.org on 2 February 2009. DOI: 10.2337/db07-1016.

Diabetes increases a women's risk to give birth to a child with a congenital malformation. Newborns of mothers suffering from type 1 diabetes have a two- to sixfold higher risk of developing congenital malformations (1–3), while that of children from women with type 2 diabetes is raised with a factor of 3–11 (4–6). The majority of these malformations concern the cardiovascular system. Epidemiological studies indicate that maternal diabetes is one of the most important risk factors for the development of congenital heart disease (CHD) (7). Considering the rapid increase of pregnant women with diabetes, the occurrence of maternal diabetes–induced CHD is a serious and increasing health problem.

How maternal diabetes induces CHD still remains to be elucidated. We have studied the involvement of two mechanisms causing complications in adult diabetic patients, being glycation and disturbance of vascular endothelial growth factor (VEGF) levels, assuming that these might also harm embryonic tissues and could thereby disturb embryonic cardiovascular development.

The formation and accumulation of advanced glycation end products (AGEs) such as N^{ε}(carboxymethyl)lysine (CML) and methylglyoxal (MG) adducts are important pathophysiological mechanisms in the development of cardiovascular complications in diabetic patients (8). Accumulation of AGEs has been reported in diabetic patients suffering from micro- and macrovascular complications and delayed wound healing (9,10) as well as in diabetic rat models (11,12). In patients, the occurrence of the complications could be prevented using pharmacological inhibitors of AGE formation such as aminoguanidine (13,14), emphasizing the importance of this mechanism in the development of diabetes complications. In rat embryos cultured in high-glucose medium, an increase in a major precursor in the formation of AGEs, i.e., 3-deoxyglucasone, was observed (10), indicating a role for glycation in the development of congenital malformations. Indeed, high values of A1C during pregnancy do not only indicate suboptimal glycemic control, they are also related to the incidence of congenital malformations (15). If their levels in pregnant women become high (A1C >14.4), malformations are identified in 40% of the neonates (16).

To study the impact of glycation on cardiovascular development, we investigated the presence of the AGEs

CML and MG adducts in embryos derived from diabetic and nondiabetic rats. We used Sprague-Dawley–derived outbred U (Uppsala) rats, previously noted for a high rate of congenital malformations in response to maternal diabetes (17,18). In addition, we used embryos of the L and B inbred rat strains derived from U and H rats, respectively. In the latter strain, diabetic pregnancy did not increase congenital malformations in the offspring.

A second strong candidate for a role in maternal diabetes–induced CHD is VEGF. For normal embryonic and cardiovascular development, it is essential that VEGF is maintained between critical threshold levels. Mice missing only one allele die at E10.5, displaying abnormal vessels (19), while also a two- to threefold overexpression of VEGF results in severe cardiovascular malformations (20). Malformations of the cardiac outflow tract, such as Tetralogy of Fallot, that are increased in the offspring of diabetic women can be induced by selective knockout of both the $VEGF_{188}$ and $VEGF_{164}$ isoforms in murine embryos and are related to a local increase of the $VEGF_{120}$ isoform and VEGF signaling in the heart (21,22).

Culture of young mouse embryos (E7.5 until E9.5) in elevated glucose levels resulted in abnormal development of the vitelline circulation. This phenomenon could be prevented by the addition of VEGF (23), suggesting that the effect of elevated glucose on vascular development is mediated by a downregulation of VEGF. Furthermore, VEGF plays a role in vascular complications in adults with diabetes (24), underscoring the importance of fine balanced VEGF levels for vascular tissue.

We studied VEGF expression locally in the developing heart using in situ hybridization on sections of rat embryos from dams with or without diabetes.

Disturbance of Smad2 signaling in the fourth pharyngeal arch artery (PAA) has been linked to arch malformations in the transforming growth factor (TGF)-β knockout mice model (25). Because both glycation and VEGF influence signaling via Smad2 (26,27), we decided to additionally study the presence of the phosphorylated Smad2 in these embryos.

RESEARCH DESIGN AND METHODS

Animals. The Uppsala Regional Ethical Committee on Animal Experiments approved the research protocol including all experimental procedures involving animals. We used 3-month-old rats from a local colony of outbred U (Uppsala) Sprague-Dawley rats, previously noted for a high rate of congenital malformations in response to maternal diabetes (17,18) as well as the L and B inbred rat strains derived from the U and H rats (a Sprague-Dawley rat strain more resistant to diabetes-induced congenital malformations), respectively. All rats were fed a commercial pellet diet (AB Analycen, Lidköping, Sweden) and had free access to food and tap water. They were maintained at an ambient temperature of 22°C with a 12-h light-dark cycle. Introduction of diabetes in female rats was performed by injecting 40 mg/kg streptozotocin (Sigma-Aldrich, Uppsala, Sweden) into the tail vein 1 week before mating commences, i.e., 1–3 weeks before conception. A state of manifest diabetes (MD) was confirmed 1 week after the injection by the presence of a blood glucose level exceeding 20 mmol/l (Medisense Glucose Sensor; Abbot Scandinavia AB, Solna, Sweden). The induced level of hyperglycemia was similar between rats of the susceptible and resistant strains. Diabetic and nondiabetic (ND) females were caged with males overnight, and conception was verified by the presence of sperm in a vaginal smear. The day of a positive vaginal smear was designated gestational day 0. Pregnancy was interrupted on gestational day 13, 14, and 16. Embryos and fetuses were fixed in 4% PBS paraformaldehyde, subsequently dehydrated in graded ethanol, transferred to xylene, and finally embedded in paraffin. Cardiac morphology was analyzed in E16 embryos from diabetic (MD) L rats ($n = 19$) and E16 embryos from B-MD dams ($n = 16$). Data were compared with the U strain embryos, which we have studied before on both E16 and E18 (18). A total of 24 E13 embryos from MD and ND dams were used for the analysis of CML and MG adduct formation and detection of phosphorylated Smad2, being L-ND ($n = 4$), L-MD ($n = 4$), B-ND ($n = 4$), B-MD ($n = 4$), U-ND ($n = 4$), and U-MD ($n = 4$). At E14, we studied 13 embryos of L-ND ($n = 2$), L-MD ($n = 2$), U-ND ($n = 6$), and U-MD ($n = 3$).

Detection of CML and MG adducts. Embryos were serially sectioned at 5 μm. Alternated sections were rehydrated and antigen retrieval was performed using the microwave to enhance staining. Sections were incubated for 1 h at room temperature with a 1:500 dilution of the anti-CML antibody and 1:5 dilution of the antibody directed against MG adducts (28,29). Subsequently, sections were washed in PBS and incubated for 60 min with a 1:200 diluted biotinylated horse anti-mouse antibody (ABC Kit; Vector Laboratories, Burlingame, CA) and incubated with ABC according to the recommendations of the manufacturer.

Detection of phosphorylated Smad2. Immunohistochemistry was performed after the protocol described above, although no microwave enhancement was performed, and the incubation of the sections, with a 1:1,000 dilution of the phosphorylated Smad2 antibody (provided by Prof. Dr. P ten Dijke, Leiden University Medical Centre, Leiden, the Netherlands), was preceded by a blocking step using 10% normal goat serum in PBS.

VEGF in situ hybridization. Consecutive transverse sections of 5 μm were rehydrated and post-fixed in 4% paraformaldehyde for 20 min. Subsequently, they were treated with 20 μg/ml Proteinase K (Promega, Leiden, the Netherlands) and 4% paraformaldehyde and by 0.1 mol/l triethanolamine-HCl (pH 8.0) + 0.25% acetic anhydride. After dehydration, sections were hybridized overnight at 55°C using sense and anti-sense ^{35}S-radiolabeled VEGF-A RNA probes that were transcribed using a 451-bp *Eco*RI/*Bam*HI cDNA clone encoding for the mouse VEGF-120 isoform (pVEGF2; provided by Dr. G. Breier, University of Technology, Dresden, Germany). The following morning, the sections were washed and then coated with Ilford G5 emulsion (Ilfort, Mobberly, U.K.), in which they were kept at 4°C for 10 days. Finally, the sections were developed in Kodak D19 (Kodak, Chalon s. Saonne, France) solution for 4 min, washed, and fixated in Ilford Hypam (Ilfort), counterstained with hematoxylin, and mounted with Pertex (Histolab Products, Goteborg, Sweden). The sections were examined by light microscopy using dark field optics.

Reconstructions. The Amira V3.1 software package (Template Graphics Software, San Diego, CA) was used to make three-dimensional reconstructions of day 13 embryos. For the reconstruction, we used 5-μm sections every 25 μm. Via manual drawing, the cardiovascular lumen and CML^+ areas were color-labeled and rendered for three-dimensional visualization. Embryos were processed under comparable conditions described above, allowing for a direct comparison of the reconstructions.

RESULTS

To identify the potential of AGEs in the development of diabetes-induced CHD, we analyzed the presence and localization of CML and MG adducts in E13 and E14 embryos from the malformation-prone L and U rat strains and the resistant B rats with (MD) and without (ND) diabetes.

At E13, CML was identified in all the MD offspring of the malformation-susceptible rats L-MD and U-MD (Fig. 1). The CML^+ area was identified in the PAAs (Fig. 1*B* and *D*). More precisely, it overlapped with segments derived from the fourth and sixth PAA and extended just proximal to the connection to the subclavian arteries. This we have shown in the three-dimensional reconstruction of the developing cardiovascular system of an E13 L-MD embryo (Fig. 2*B–D*) and its schematic representation indicating the various PAA segments (Fig. 2*A*). Formation of CML also occurred in the vessel wall of the ascending aorta and pulmonary trunk, where staining was more intense in the aortic wall than in the pulmonary trunk (compare Fig. 2*C* to Fig. 2*D*). Furthermore, CML^+ cells were identified in the outflow tract myocardium bordering the cushions of the outflow tract (Fig. 2*B*, *blue*). CML accumulated in the cytoplasm rather than in the extracellular matrix. No CML could be detected in any of the E13 offspring of the L-ND or in MD or ND embryos derived from the malformation-resistant B strain (Fig. 3). In embryos of U-ND rats, we observed a weak CML staining (Fig. 1). Using immunohis-

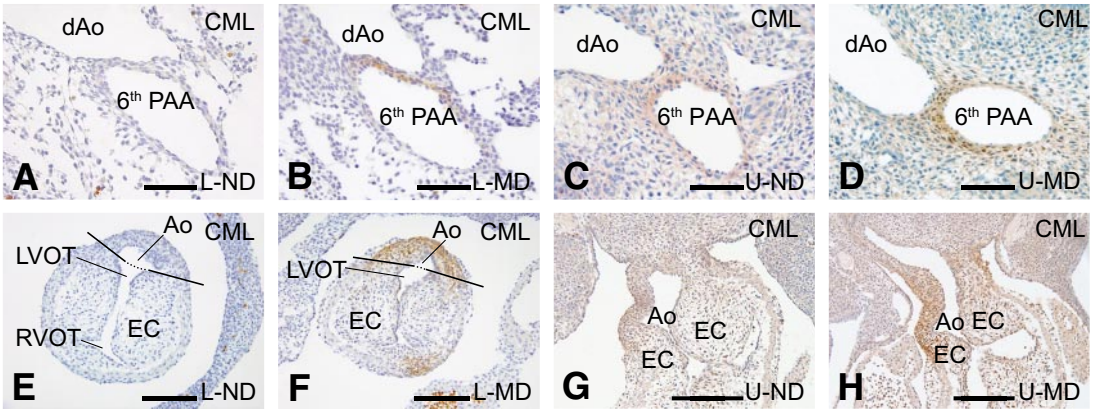

FIG. 1. CML detection in E13 embryos of the susceptible L and U strain. Immunohistochemical detection of CML is shown in sections derived from the offspring of rats of the susceptible L and U strain being either nondiabetic (ND) or diabetic (MD). *A–D* are at the level of the PAA. In *E–H*, we can see the presence of CML in the outflow tract (which is not yet septated at this stage of development). Ao, aorta; dAo, descending aorta; EC, endocardial cushions; LVOT, left ventricular outflow tract; RVOT, right ventricular outflow tract. Scale bars in *A–F*, 60 μm; in *G* and *H*, 200 μm. (A high-quality digital representation of this figure is available in the online issue.)

tochemical analysis, no MG adducts could be detected in any of the embryos at this stage.

At E14, CML was detected in all embryos in the proximal outflow tract myocardium, in the ascending aorta, all PAAs, the subclavian arteries, the dorsal aorta, the pulmonary trunk, and the pulmonary arteries. CML was also present in the cushions of the outflow tract, where it was increased in the MD offspring of the U and L rats (Fig. 4*B*, *D*, and *F*), compared with that in ND embryos or MD embryos of the resistant B rats (Fig. 4*A*, *C*, and *E*). Again no MG adducts could be detected using immunohistochemical analysis.

As hyperglycemia influences VEGF expression and alterations in the amount of VEGF can disturb cardiovascular development, we performed VEGF in situ hybridizations in embryos from ND and MD dams. At E13, a high expression of VEGF was seen in all myocardial cells aligning the endocardial cushions of both the inflow tract and the outflow tract of the heart, the myocardial cells in the ventricular septum, and the fibrous tissue protruding into the base of the atrial septum, the so-called spina vestibuli. At this stage of development, VEGF expression was similar in both ND and MD embryos of L, U, or B rats. E14 ND embryos and the MD embryos of the resistant B

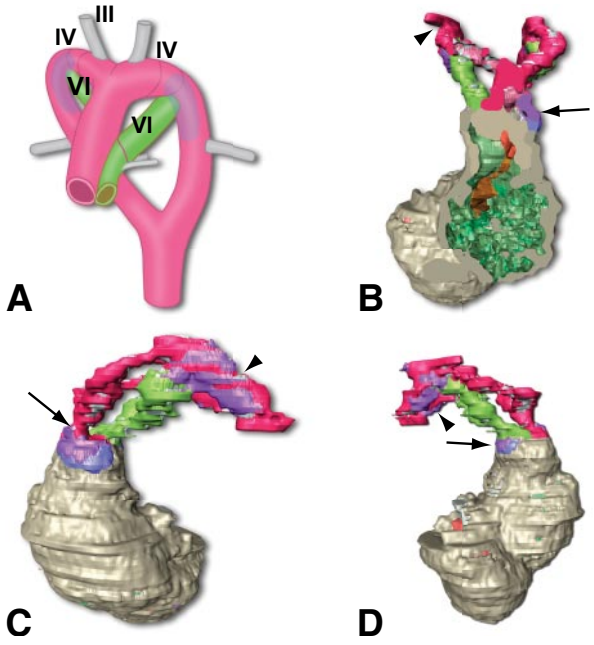

FIG. 2. Indication of the localization of CML in a three-dimensional reconstruction of an E13 embryo from a diabetic L rat. In this Amira reconstruction (*B–D*), the position of CML is indicated in purple (when present in the vessel wall) or blue (when present in the myocardium of the outflow tract). The aorta is indicated in red, the pulmonary trunk and ductus arteriosus in green, and the myocardium in gray. The frontal plane (*B*) illustrates that the CML$^+$ area is partly located in the myocardium, the outflow tract (attached to the endocardial cushion) indicated in blue, and partly in the vessel wall of the ascending aorta indicated in purple. The view from the left (*C*) shows the CML$^+$ area on the aortic side of the outflow tract (arrow) as well as in the PAA (arrowhead). The view from the right side (*D*) shows the presence of CML on the pulmonary side of the outflow tract (arrow) and in the right-sided PAA (arrowhead). In the artist's impression (*A*), the location of the third PAA (future carotic artery), the fourth PAA (the left-sided fourth will become part of the aortic arch and the right-sided fourth will be part of the brachial cephalic artery), and the sixth PAA (ductus arteriosus) are indicated. The transparent purple indicates the CML$^+$ area. (A high-quality digital representation of this figure is available in the online issue.)

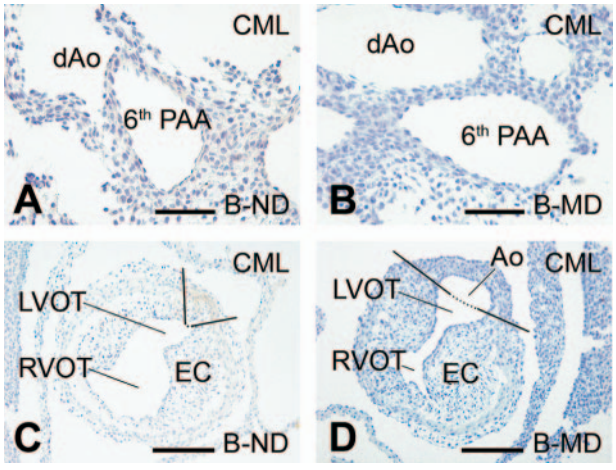

FIG. 3. CML detection in the resistant B strain embryos at E13. Immunohistochemical shows that there is no CML accumulation in sections derived from the offspring of rats from the resistant B strain being either nondiabetic (ND) or diabetic (MD). Sections *A* and *B* are at the level of the PAA and in *C* and *D* at the outflow tract (which is not yet septated at this stage of development). Ao, aorta; dAo, descending aorta; EC, endocardial cushions; LVOT, left ventricular outflow tract, RVOT, right ventricular outflow tract. Scale bar = 60 μm. (A high-quality digital representation of this figure is available in the online issue.)

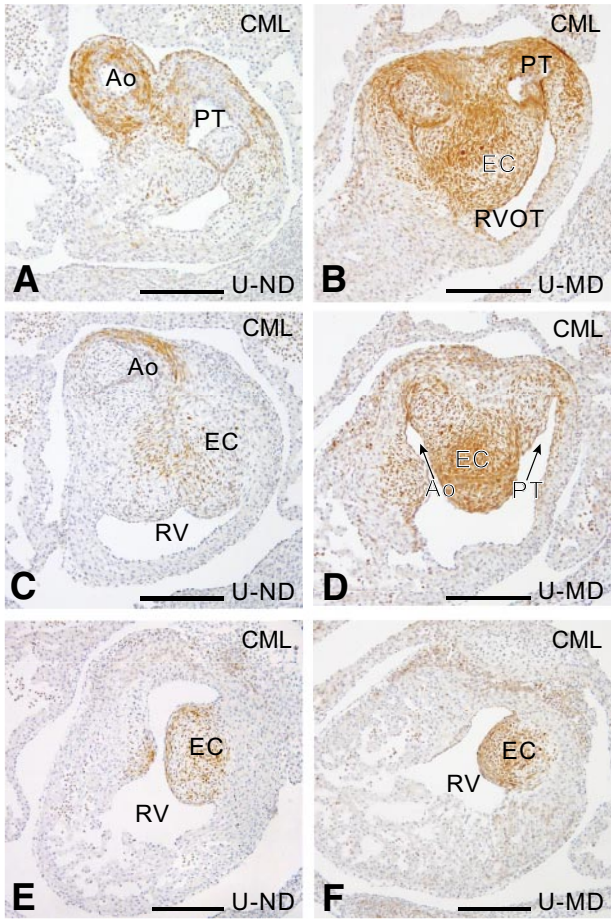

FIG. 4. CML detection in E14 embryos. Sections at several levels in the endocardial cushions of the outflow tract show an increase in CML in the U-MD (*B*, *D*, and *F*) compared with the U-ND (*A*, *C*, and *E*) offspring. Ao, aorta; PT, pulmonary trunk; EC, endocardial cushion; RV, right ventricle; RVOT, right ventricular outflow tract. Scale bar = 200 μm. (A high-quality digital representation of this figure is available in the online issue.)

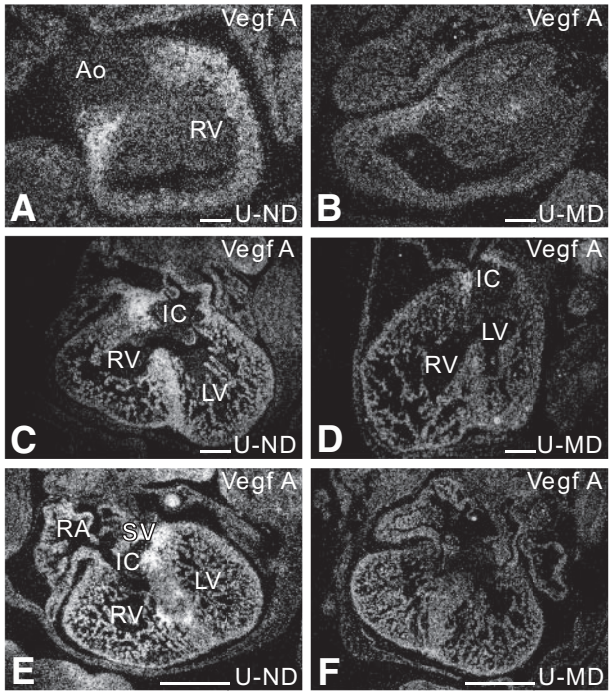

FIG. 5. Diabetes-induced decrease in cardiac VEGF expression as shown by in situ hybridization. In the E14-ND offspring, VEGF is abundantly expressed in the myocardium aligning the cushions of the outflow tract of the heart (*A*), in the ventricular septum (*C*), and in the myocardium around the cushions of the inflow tract of the heart (*C* and *E*). At E14, we see a diabetes-induced decrease in VEGF expression in all L-MD embryos ($n = 2$) and in 75% of the four-unit MD embryos ($n = 4$) in the myocardium aligning the cushions of the outflow (*B*) and inflow tract of the heart (*D* and *F*), in the ventricular septum (*D*). Ao, aorta; IC, inflow tract cushion; LV, left ventricle; RA, right atrium; RV, right ventricle; SV, sinus venosus. Scale bar = 200 μm.

strain showed a VEGF mRNA expression pattern similar to that seen on E13. However, a diabetes-induced decrease in VEGF expression was observed in five of six MD embryos derived from the malformation-prone L and U strain. This decrease in VEGF could be observed in all areas that normally have a high VEGF expression level (Fig. 5).

Because both glycation products and VEGF influence the Smad2 signaling, we analyzed active Smad2 using an antibody against phosphorylated Smad2. At E13, phosphorylated Smad2 was increased in the CML^+ positive vessel wall of the ascending aorta and pulmonary trunk as well as in the myocardium of the outflow tract (Fig. 6*D*) in L and U MD embryos, compared with either the surrounding CML^- cells or to the same area from MD-B embryos (Fig. 6*B*) or ND offspring. In the PAAs of all embryos, the level of phosphorylated Smad2 was relatively high compared with other arteries without a clear distinction for CML^+ or CML^- areas.

At E14, phosphorylation of Smad2 overlapped with the increased CML patterning, which in this stage of development was present in the cushions of the outflow tract of the heart (Fig. 6*F–H*). In addition, phosphorylated Smad2 is higher in the cushions of the E14 MD offspring (Fig. 6*H*) than in the ND offspring (Fig. 6*F*).

The L and B strains are inbred rat strains of which the L strain is known to present with extra-cardiac malformations such as micrognatia, cleft palet, or skeletal malformations, whereas the B strain is more resistant to these malformations. Cardiovascular anomalies have not been described in these strains. It was not known if the diabetes-induced facial anomalies were linked to cardiovascular malformations. We have therefore studied cardiac morphology of E16 L-MD and B-MD embryos and compared the identified malformations with those we have previously characterized in the U strain embryos of E16 and E18 (18). In the inbred L rats, all MD fetuses had a CHD compared with 67% in the outbred U-MD offspring. Outflow tract anomalies were identified in 74% of the L-MD offspring compared with 63% in the U-MD offspring. Defects of the fourth PAA were seen in 47% of the L-MD and 22% of the U-MD embryos and sixth PAA defects in 21% of the L-MD and 11% of the U-MD embryos (Table 1). In the B-MD offspring resistant to the maternal diabetes–induced extra-cardiac malformations, the number of cardiovascular malformations is also considerably lower (Table 1). From these data, we can conclude that the L rat strain is susceptible to diabetes-induced CHD comparable to the U rat strain.

DISCUSSION

At E13, CML accumulation appeared in a small area of the developing outflow tract and in the PAAs in MD embryos of the susceptible L and U strains. At this developmental stage, the PAAs are still paired and their remodeling has not yet started (18). The addition of myocardium from the secondary heart field to the primary heart tube is almost

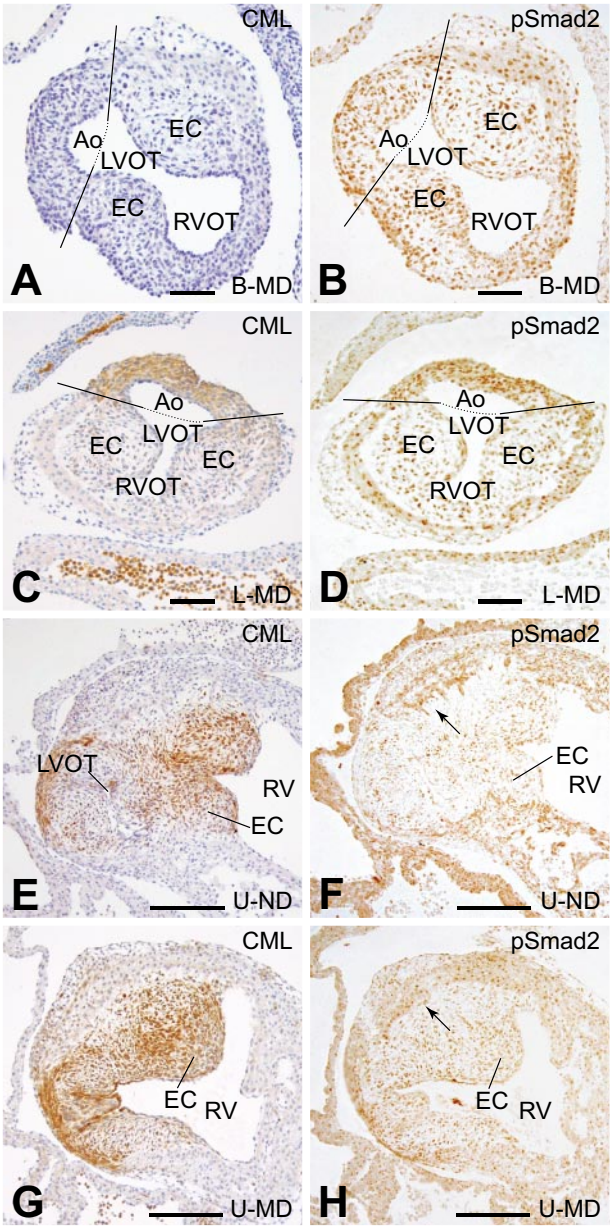

FIG. 6. (Co)localization of CML and phosphorylated Smad2. In this figure, we show the (co)localization of CML and phosphorylated Smad2 in the developing cardiovascular system. At E13, no CML (*A*) and no increase in phosphorylated Smad2 (*B*) were observed in the outflow tract of the B-MD offspring. In the MD offspring of the susceptible L strain, both CML (*C*) and phosphorylated Smad2 (*D*) were increased in the outflow tract of the heart. At E14, CML is identified in the endocardial cushions, although more CML is identified in the U-MD offspring (*G*) compared with the U-ND offspring (*E*). At the same time, phosphorylated Smad2 is increased in the cushions of the outflow tract in embryos of the MD offspring (*H*) compared with those from nondiabetic dams (*F*). Scale bar in *A–D* = 60 μm and in *E–H* = 200 μm. (A high-quality digital representation of this figure is available in the online issue.)

completed, and outflow tract septation is in process (30). The cells positive for CML on E13 are known to originate from two cell populations. The most proximal CML^+ cells are secondary heart field–derived cells that have migrated from the splanchnic mesoderm (31,32). The other CML^+ cells in the ascending aorta and PAA are derived from the cardiac neural crest cells (32–35). Given the temporal spatial overlap between CML accumulation and the development of cardiovascular outflow and PAA anomalies, it can be postulated that both the addition of myocardium from the secondary heart field and the function of neural crest cells are hampered in diabetic pregnancies (17,18,36–38).

TABLE 1
Percentage (numbers) of congenital heart defects in the offspring of diabetic rats from the susceptible U and L strain and the resistant B strain

	n	Normal	Outflow tract defects	Fourth PAA defects	Sixth PAA defects
U-MD	27	37% (9/27)	63% (17/27)	22% (6/27)	11% (3/27)
L-MD	19	0% (0/19)	74% (14/19)	47% (9/19)	21% (4/19)
B-MD	16	81% (13/16)	13% (2/16)	6% (1/16)	0% (0/16)

L-MD and B-MD fetuses were all of E16; the U-MD fetuses were of E16 and E18 (18).

The accumulation of CML and the increase in phosphorylated Smad2 at E13 is asymmetric, being higher on the aortic side than on the side of the pulmonary trunk. This is exactly opposite to the lacZ expression identified in the y96-Myf5-nLacZ-16 transgenic mice, which is predominantly seen on the side of the pulmonary trunk (39). From this, Bajolle et al. (39) hypothesize that deviations from the left/right asymmetry inhibits outflow tract rotation and result in anomalies such as a double outlet right ventricle. Analogous and asymmetric increase in CML accumulation might disturb the left/right signaling in MD embryos and subsequently the rotation of the outflow tract, also resulting in CHD, such as a double outlet right ventricle that is frequently seen in our MD offspring (18). Furthermore, embryos that are heterozygous for both a *Smad2* and *nodal* mutation (40) show defects in left-right patterning, resulting in abnormal cardiac looping. This indicates that also the asymmetric increase in phosphorylated Smad2 (co-localizing with the asymmetric CML increase) in the E13 MD embryos is likely to play a role in diabetes-induced congenital heart malformations.

At E14, septation is almost completed and the process of PAA remodeling is still in progress. Although CML could be detected in the embryonic vasculature in both MD and ND offspring of all strains, increased CML was found in the cushions of the outflow tract in the MD offspring of the susceptible U and L dams. Abnormal cushions as seen on E14 could lead to congenital heart malformations such as Tetralogy of Fallot or double outlet right ventricle. We have previously identified these malformations in combination with hypoplastic cushions in the MD offspring of these rats (18), in which we now show an increase in CML.

CML is an AGE that can be formed on lysine residues in proteins by a glycoxidation reaction (41). In the embryos of our study, we failed to detect MG adducts, which are produced from a glycation reaction. This raises the question whether the CML accumulation indicates an increase in the formation of AGEs or an increase in oxidative stress. MG adducts–mediated formation of nonenzymatic glycation did not take place in sufficient amounts. It cannot be ruled out that other AGEs, which are not detected by the antibodies used in this study, may play a role in the formation of CHD. However, we favor the explanation that, in our model, the increase in CML can be used as a biomarker for oxidative damage, as has been suggested before (41,42). We base this opinion on the fact that antioxidant supplementation reduces the number and severity of the diabetes-induced CHD in the offspring of these rats (17). In addition, increasing the oxidative stress by injection of antimycin A in pregnant mice results in

similar CHD, as seen in the offspring of diabetic mice (43), an effect that could be diminished by antioxidant supplementation. Furthermore, CHD was reduced by the addition of antioxidant in chicken embryos in which neural crest cells were exposed to elevated glucose (37). Next to these experimental models, it has been shown that women who gave birth to a child with a CHD have higher levels of biomarkers for oxidative stress (44). On the basis of these data, we are convinced that a local glucose-induced increase in oxidative stress, as pointed out by CML, is an important mechanism in the development of congenital malformations in the offspring from diabetic pregnancies.

Elevated glucose levels can disturb the cardiovascular development by influencing the expression of VEGF (45). The addition of high glucose concentrations to cultured mice embryos inhibits endothelial to mesenchymal transformation in the endocardial cushions by a reduction of VEGF levels (45). In the MD embryos, a clear overlap between CML accumulation, reduced VEGF expression, and hypoplastic endocardial outflow tract cushions was identified. We assume that a decrease in VEGF causes cushion hypoplasia and the related maldevelopment of the outflow tract (double outlet right ventricle and Tetralogy of Fallot). In addition to our results, decreased levels of VEGF were identified in cultured embryos and in vitro endocardial cushions after exposure to elevated glucose (23,45). This negative relation between diabetes and VEGF expression in the embryo that we and others found is opposite to data for adult endothelial cells (46,47).

At E14 in the endocardial cushions of the outflow tract of the heart, CML and phosphorylated Smad2 were increased, whereas VEGF expression was decreased. AGEs can induce Smad2 phosphorylation in vitro and in vivo (26), and therefore CML might be responsible for the raise in phosphorylated Smad2. However, VEGF has been reported to inhibit Smad2 phosphorylation (48); therefore, a reduced level of VEGF in these structures could also relate to the identified increase in Smad2 phosphorylation. Although endothelial to mesenchymal transformation can be increased by TGFβ/Smad2 signaling (49,50), the hypoplastic appearance of the outflow cushions contradicts this assumption. We assume that the lack of myocardial VEGF expression is more detrimental for cushion development than the stimulating effect one might expect from Smad2. Unfortunately, the pathways for activation and action of Smad2 are complex, involving interactions with multiple players, and at this time, it is not possible to fully elucidate them.

The incidence of full-blown CHD in fetuses (>E16) between the L and U strain clearly reveals their genetic predisposition for diabetes-induced congenital cardiovascular malformations. The high percentage of CHD in the MD offspring of the inbred L strain, for which rats were selected on the basis of extra-cardiac malformations, implies that there is a link between cardiovascular and noncardiac congenital malformations. The similarity between the number and type of malformations identified in the L-MD and U-MD fetuses justifies the use of the L strain next to the U strain for the identification of the pathways involved in diabetes-induced CHD.

In this research, we have provided a novel proof for a specific temporal-spatial pattern rather than a general increase in CML accumulation, suggesting a raise in oxidative stress. The increase in CML and phosphorylated Smad2 strikingly overlapped with those cardiovascular regions that are at high risk during development. Furthermore, the hyperglycemia-related decrease in VEGF was observed in the same regions. We postulate that local rather than general changes in CML accumulation, Smad2 phosphorylation, and VEGF expression are detrimental for the developing cardiovascular system in MD embryos.

ACKNOWLEDGMENTS

This work was funded by the Netherlands Heart Foundation grants NHS2002B035 and NHS2006B074, the Ernfors Family Fund, the Swedish Diabetes Association, and the Swedish Research Council Grant 12X-7475.

This work was also funded by the Novo Nordisk Foundation. No other potential conflicts of interest relevant to this article were reported.

We would like to thank P ten Dijke for the gift of the antibody raised against phosphorylated Smad2. We also thank Jan Lens for graphics and layout.

Parts of this study were presented at the 4th International Symposium on Diabetes and Pregnancy, 29–31 March 2007, Istanbul, and at the 12th Annual Weinstein Cardiovascular Development Conference, 19–22 May 2005, Tucson, Arizona.

REFERENCES

1. Eriksson UJ, Cederberg J, Wentzel P. Congenital malformations in offspring of diabetic mothers: animal and human studies. Rev Endocr Metab Disord 2003;4:79–93
2. Dunne FP, Chowdhury TA, Hartland A, Smith T, Brydon PA, McConkey C, Nicholson HO. Pregnancy outcome in women with insulin-dependent diabetes mellitus complicated by nephropathy. QJM 1999;92:451–454
3. Loffredo CA, Wilson PD, Ferencz C. Maternal diabetes: an independent risk factor for major cardiovascular malformations with increased mortality of affected infants. Teratology 2001;64:98–106
4. Homko CJ, Reece EA. Development of early-onset type 2 diabetes in the young: implications for child bearing. Curr Diabetes Rep 2003;3:313–318
5. Hieronimus S, Fenichel P. Pregnancy in women with type 2 diabetes: an uncertain prognosis. Diabetes Metab 2004;30:281–284
6. Dunne F, Brydon P, Smith K, Gee H. Pregnancy in women with type 2 diabetes: 12 years outcome data 1990–2002. Diabet Med 2003;20:734–738
7. Ferencz C, Rubin JD, Mccarter RJ, Brenner JI, Neill CA, Perry LW, Hepner SI, Downing JW. Congenital heart disease: prevalence at livebirth: the Baltimore Washington Infant Study. Am J Epidemiol 1985;121:31–36
8. Brownlee M. The pathobiology of diabetic complications: a unifying mechanism. Diabetes 2005;54:1615–1625
9. Ahmed N. Advanced glycation endproducts: role in pathology of diabetic complications. Diabetes Res Clin Pract 2005;67:3–21
10. Eriksson UJ, Wentzel P, Minhas HS, Thornalley PJ. Teratogenicity of 3-deoxyglucosone and diabetic embryopathy. Diabetes 1998;47:1960–1966
11. van Deutekom AW, Niessen HW, Schalkwijk CG, Heine RJ, Simsek S. Increased nepsilon-(carboxymethyl)-lysine levels in cerebral blood vessels of diabetic patients and in a (streptozotocin-treated) rat model of diabetes mellitus. Eur J Endocrinol 2008;158:655–660
12. Lu MP, Wang R, Song X, Wang X, Wu L, Meng QH: Modulation of methylglyoxal and glutathione by soybean isoflavones in mild streptozotocin-induced diabetic rats. *Nutr Metab Cardiovasc Dis* 2008;18:618–623
13. Hammes HP, Martin S, Federlin K, Geisen K, Brownlee M. Aminoguanidine treatment inhibits the development of experimental diabetic retinopathy. Proc Natl Acad Sci U S A 1991;88:11555–11558
14. Cameron NE, Gibson TM, Nangle MR, Cotter MA. Inhibitors of advanced glycation end product formation and neurovascular dysfunction in experimental diabetes: Maillard Reaction: chemistry at the Interface of Nutrition, Aging, and Disease. 2005;1043:784–792
15. Miller E, Hare JW, Cloherty JP, Dunn PJ, Gleason RE, Soeldner JS, Kitzmiller JL. Elevated maternal hemoglobin A1c in early pregnancy and major congenital anomalies in infants of diabetic mothers. N Engl J Med 1981;304:1331–1334
16. Greene MF, Hare JW, Cloherty JP, Benacerraf BR, Soeldner JS. First-trimester hemoglobin A1 and risk for major malformation and spontaneous abortion in diabetic pregnancy. Teratology 1989;39:225–231
17. Siman CM, Gittenberger-De Groot AC, Wisse B, Eriksson UJ. Malformations in offspring of diabetic rats: morphometric analysis of neural

crest-derived organs and effects of maternal vitamin E treatment. Teratology 2000;61:355–367
18. Molin DGM, Roest PAM, Nordstrand H, Wisse LJ, Poelmann RE, Eriksson UJ, Gittenberger-de-groot AC: Disturbed morphogenesis increased rate of cardiac outflow tract and aortic arch anomalies in the offspring of diabetic rats. Birth Defects Res A Clin Mol Teratol 2004;70:927–938
19. Carmeliet P, Ferreira V, Breier G, Pollefeyt S, Kieckens L, Gertsenstein M, Fahrig M, Vandenhoeck A, Harpal K, Eberhardt C, Declercq C, Pawling J, Moons L, Collen D, Risau W, Nagy A. Abnormal blood vessel development and lethality in embryos lacking a single VEGF allele. Nature 1996;380: 435–439
20. Miquerol L, Langille BL, Nagy A. Embryonic development is disrupted by modest increases in vascular endothelial growth factor gene expression. Development 2000;127:3941–3946
21. Stalmans I, Lambrechts D, De Smet F, Jansen S, Wang J, Maity S, Kneer P, von der OM, Swillen A, Maes C, Gewillig M, Molin DG, Hellings P, Boetel T, Haardt M, Compernolle V, Dewerchin M, Plaisance S, Vlietinck R, Emanuel B, Gittenberger-de-groot AC, Scambler P, Morrow B, Driscol DA, Moons L, Esguerra CV, Carmeliet G, Behn-Krappa A, Devriendt K, Collen D, Conway SJ, Carmeliet P. VEGF: a modifier of the del22q11 (DiGeorge) syndrome? Nat Med 2003;9:173–182
22. van den Akker NM, Molin DG, Peters PP, Maas S, Wisse LJ, van Brempt R, van Munsteren CJ, Bartelings MM, Poelmann RE, Carmeliet P, Gittenberger-De Groot AC. Tetralogy of fallot and alterations in vascular endothelial growth factor-A signaling and notch signaling in mouse embryos solely expressing the VEGF120 isoform. Circ Res 2007;100:842–849
23. Pinter E, Haigh J, Nagy A, Madri JA. Hyperglycemia-induced vasculopathy in the murine conceptus is mediated via reductions of VEGF expression and VEGF receptor activation. Am J Pathol 2001;158:1199–1206
24. Aiello LP, Wong JS. Role of vascular endothelial growth factor in diabetic vascular complications. Kidney Int 2000;58:S113–S119
25. Molin DGM, Poelmann RE, DeRuiter MC, Azhar M, Doetschman T, Gittenberger-De Groot AC. Transforming growth factor beta-SMAD2 signaling regulates aortic arch innervation and development. Circ Res 2004; 95:1109–1117
26. Li JH, Huang XR, Zhu HJ, Oldfield M, Cooper M, Truong LD, Johnson RJ, Lan HY. Advanced glycation end products activate Smad signaling via TGF-beta-dependent and -independent mechanisms: implications for diabetic renal and vascular disease. FASEB J 2003;17:176–178
27. Yamauchi K, Nishimura Y, Shigematsu S, Takeuchi Y, Nakamura J, Aizawa T, Hashizume K. Vascular endothelial cell growth factor attenuates actions of transforming growth factor-beta in human endothelial cells. J Biol Chem 2004;279:55104–55108
28. Fa MLM, Schalkwijk CG, Engelse M, van Hinsbergh VWM. Interaction of N epsilon(carboxymethyl)lysine- and methylglyoxal-modified albumin with endothelial cells and macrophages: splice variants of PAGE may limit the responsiveness of human endothelial cells to AGEs. Thromb Haemost 2006;95:320–328
29. Schalkwijk CG, Baidoshvili A, Stehouwer CDA, van Hinsbergh VWM, Niessen HWM. Increased accumulation of the glycoxidation product N-epsilon-(carboxymethyl)lysine in hearts of diabetic patients: generation and characterisation of a monoclonal anti-CML antibody. Biochim Biophys Acta 2004;1636:82–89
30. Kelly RG. Molecular inroads into the anterior heart field. Trends Cardiovasc Med 2005;15:51–56
31. Cai CL, Liang XQ, Shi YQ, Chu PH, Pfaff SL, Chen J, Evans S. Isl1 identifies a cardiac progenitor population that proliferates prior to differentiation and contributes a majority of cells to the heart. Dev Cell 2003;5:877–889
32. Waldo KL, Hutson MR, Stadt HA, Zdanowicz M, Zdanowicz J, Kirby ML. Cardiac neural crest is necessary for normal addition of the myocardiurn to the arterial pole from the secondary heart field. Dev Biol 2005;281:66–77
33. Jiang X, Rowitch DH, Soriano P, McMahon AP, Sucov HM. Fate of the mammalian cardiac neural crest. Development 2000;127:1607–1616
34. Epstein JA, Li J, Lang D, Chen F, Brown CB, Jin FZ, Li MM, Thomas M, Liu ECJ, Wessels A, Lo CW. Migration of cardiac neural crest cells in Splotch embryos. Development 2000;127:1869–1878
35. Bergwerff M, Verberne ME, DeRuiter MC, Poelmann RE, Gittenberger-De Groot AC. Neural crest cell contribution to the developing circulatory system: implications for vascular morphology? Circ Res 1998;82:221–231
36. Cederberg J, Picard JJ, Eriksson UJ. Maternal diabetes in the rat impairs the formation of neural-crest derived cranial nerve ganglia in the offspring. Diabetologia 2003;46:1245–1251
37. Roest PA, van IL, Vis S, Wisse LJ, Poelmann RE, Steegers-Theunissen RP, Molin DG, Eriksson UJ, Gittenberger-De Groot AC. Exposure of neural crest cells to elevated glucose leads to congenital heart defects, an effect that can be prevented by N-acetylcysteine. Birth Defects Res A Clin Mol Teratol 2007;79:231–235
38. Suzuki N, Svensson K, Eriksson UJ. High glucose concentration inhibits migration of rat cranial neural crest cells in vitro. Diabetologia 1996;39: 401–411
39. Bajolle F, Zaffran S, Kelly RG, Hadchouel J, Bonnet D, Brown NA, Buckingham ME. Rotation of the myocardial wall of the outflow tract is implicated in the normal positioning of the great arteries. Circ Res 2006;98:421–428
40. Nomura M, Li E. Smad2 role in mesoderm formation, left-right patterning and craniofacial development. Nature 1998;393:786–790
41. Fu MX, Requena JR, Jenkins AJ, Lyons TJ, Baynes JW, Thorpe SR. The advanced glycation end product, N-(epsilon)(carboxymethyl)lysine, is a product of both lipid peroxidation and glycoxidation reactions. J Biol Chem 1996;271:9982–9986
42. Horie K, Miyata T, Maeda K, Miyata S, Sugiyama S, Sakai H, van Ypersole de SC, Monnier VM, Witztum JL, Kurokawa K. Immunohistochemical colocalization of glycoxidation products and lipid peroxidation products in diabetic renal glomerular lesions: implication for glycoxidative stress in the pathogenesis of diabetic nephropathy. J Clin Invest 1997;100:2995–3004
43. Morgan SC, Relaix F, Sandell LL, Loeken MR. Oxidative stress during diabetic pregnancy disrupts cardiac neural crest migration and causes outflow tract defects. Birth Defects Res A Clin Mol Teratol 2008;82:453–463
44. Hobbs CA, Cleves MA, Zhao W, Melnyk S, James SJ. Congenital heart defects and maternal biomarkers of oxidative stress. Am J Clin Nutr 2005;82:598–604
45. Enciso JM, Gratzinger D, Camenisch TD, Canosa S, Pinter E, Madri JA. Elevated glucose inhibits VEGF-mediated endocardial cushion formation: modulation by PECAM-1 and MMP-2. J Cell Biol 2003;160:605–615
46. Gonzalez-Pacheco FR, Deudero JJP, Castellanos MC, Castilla MA, Alvarez-Arroyo MV, Yague S, Caramelo C. Mechanisms of endothelial response to oxidative aggression: protective role of autologous VEGF and induction of VEGFR2 by H2O2. Am J Physiol Heart Circ Physiol 2006;291:H1395–H1401
47. Yamagishi S, Yonekura H, Yamamoto Y, Katsuno K, Sato F, Mita I, Ooka H, Satozawa N, Kawakami T, Nomura M, Yamamoto H. Advanced glycation end products-driven angiogenesis in vitro. J Biol Chem 1997;272:8723–8730
48. Aoyama N, Molin DGM, Mentink MMT, Koerten HK, De Ruiter MC, Gittenberger-De Groot AC, Poelmann RE. Changing intracellular compartmentalization of beta-galactosidase in the ROSA26 reporter mouse during embryonic development: a light- and electron-microscopic study. Anat Rec A Discov Mol Cell Evol Biol 2004;279A:740–748
49. Zavadil J, Cermak L, Soto-Nieves N, Bottinger EP. Integration of TGF-beta/Smad and Jagged1/Notch signalling in epithelial-to-mesenchymal transition. EMBO J 2004;23:1155–1165
50. Davies M, Robinson M, Smith E, Huntley S, Prime S, Paterson I. Induction of an epithelial to mesenchymal transition in human immortal and malignant keratinocytes by TGF-beta 1 involves MAPK, Smad and AP-1 signalling pathways. J Cell Biochem 2005;95:918–931